Available online at www.sciencedirect.com
ScienceDirect
Journal of the European Ceramic Society 31 (2011) 2453–2458
www.elsevier.com/locate/jeurceramsoc

Effect of synthesis condition on morphology and yield of hydrothermally grown SnO_2 nanorod clusters

S. Supothina*, R. Rattanakam, S. Vichaphund, P. Thavorniti

National Metal and Materials Technology Center, 114 Thailand Science Park, Paholyothin Rd., Klong Luang, Pathumthani, 12120, Thailand

Received 30 August 2010; received in revised form 1 February 2011; accepted 11 February 2011
Available online 8 March 2011

Abstract

In this present work, we report the synthesis of SnO_2 nanorod clusters by means of hydrothermal treatment of colloidal hydrous tin oxide at 200 °C. Effect of synthesis parameters including concentrations of $Na_2SnO_3{\cdot}3H_2O$ and NaOH, and hydrothermal time on morphology and yield of the products is investigated. At optimum synthesis condition, nanorod clusters consisting of single crystalline, tetragonal-shaped rutile SnO_2 nanorod with uniform shape and size of 190 ± 6 nm in diameter and 1.4 ± 0.2 μm in length were obtained. The influence of precursor concentration on yield and morphology development was discussed. Grown mechanism is described based on aggregation of nanocrystals and their subsequent growth homocentrically.

Keywords: Grain growth; Electron microscopy; Microstructure-final; Sensors; Powder-chemical preparation

1. Introduction

Since the recognition of gas-sensing capability of a semiconducting oxide in 1960s,[1] research in this field have been widely conducted both in the aspect of materials and devices. Recently, the development of high sensitive gas sensors is of the great interest owing to the need in detection of toxic or inflammable gases in the industry and for air pollution monitoring. In principle any semiconducting oxide can be exploited as a sensor by monitoring changes of its resistance during interaction with the detected gas molecules at an operating temperature typically above 200 °C. Tin oxide (SnO_2), an n-type semiconductor with the wide band-gap of 3.6 eV, has been extensively explored for many years as a gas-sensing material due to its high sensitivity at conveniently low operating temperatures, fast response and good selectivity to different gases although lately many studies extended also to other oxides.[2–4] To take the advantage of their high surface-to-volume ratio, nanostructured SnO_2 of various morphologies such as nanorod, nanowire, nanotube, nanoflower and hollow sphere have been studied for gas-sensing performance.[5–10] Several synthetic methods such as thermal evaporation, thermal decomposition, molten-salt synthesis, sonochemical synthesis, aqueous growth and hydrothermal have been used to prepare SnO_2 nanostructures with a variety of morphologies.[11–14] Although these methods can be effective for controlling particle morphology, some drawbacks are found in some methods. For example, the complicated process of sonication procedure and the use of very high temperature of molten-salt method may not be favorable for large-scale synthesis. Recently, hydrothermal has been used widely to synthesize 1-dimensional nanostructured oxide materials since the anisotropic growth of the crystal can be favored under high pressure and temperature.

In this present work, we report the influence of synthesis condition including concentrations of precursors, hydrothermal time and temperature on morphology and yield of SnO_2 nanorods. Grown mechanism is also proposed.

2. Experimental procedure

2.1. Synthesis of SnO_2 nanorod clusters

Sodium stannate trihydrate ($Na_2SnO_3{\cdot}3H_2O$, Aldrich), sodium hydroxide (NaOH, RCI Labscan) and absolute ethanol (C_2H_5OH, RCI Labscan) were used as received. In a typical synthesis, 20 mL of absolute ethanol was slowly added into 20 mL

* Corresponding author. Tel.: +66 2 5646500; fax: +66 2 5646447.
E-mail addresses: sitthis@mtec.or.th, sitthisuntorn@hotmail.com (S. Supothina).

0955-2219/$ – see front matter © 2011 Elsevier Ltd. All rights reserved.
doi:10.1016/j.jeurceramsoc.2011.02.018

of 0.188 M [$Na_2SnO_3 \cdot 3H_2O$]/0.35 M [NaOH] aqueous solution at ambient room temperature under stirring condition. To ensure complete reaction, the mixed solution was stirred for 30 min to obtain white suspension. The suspension was transferred into a 50-mL Teflon-lined stainless steel autoclave, and held in an electric oven at 200 °C for 48 h. After cooling down to room temperature, the products were washed for at least 3 times with deionized water by vacuum filtration using a 0.1-μm cellulose membrane and finally dried at 105 °C overnight. To study the effect of precursor concentration on morphology and yield of the product, the hydrothermal synthesis was performed at various concentrations of $Na_2SnO_3 \cdot 3H_2O$ and NaOH. To further investigate a mechanism for crystal growth, morphology development at various hydrothermal times was studied.

2.2. Characterization

Crystal structure of the synthesized product was identified by using an X-ray diffractometer (XRD, JDX 3530). Microstructural analysis was performed by using scanning electron microscopes (SEM, JSM 6301F and S-3400N) and a transmission electron microscope (TEM, JEM 2010). Several isolated clusters were observed by TEM to investigate their formation mechanism. The cluster size was averaged from the size of 5 clusters measured from SEM image while the size of the nanorod was the average size of 20 nanorods lying parallel to the paper surface.

3. Results and discussion

Fig. 1 shows XRD patterns of the samples prepared from different concentration of $Na_2SnO_3 \cdot 3H_2O$ at 200 °C for 48 h. All the samples had similar XRD patterns which were identified as SnO_2 with rutile structure (JCPDS# 41-1445). Concentration of $Na_2SnO_3 \cdot 3H_2O$ solution had no effect on crystal structure of the SnO_2 nanorods at the fixed pH employed. Relative intensities of the major planes are similar to those of standard powder diffraction pattern, indicating that the samples had no preferred orientation. It has been reported that the hydrothermal-grown SnO_2 nanorods can exhibit a preferred orientation.[15] Such preferred growth is not observed in this work, possibly because of different crystallization mechanism taking place in our hydrothermal reactor.

Fig. 2 shows SEM images of the SnO_2 nanorod clusters prepared at various concentrations of $Na_2SnO_3 \cdot 3H_2O$. The morphology of the product is found to be dependent on the concentration of the $Na_2SnO_3 \cdot 3H_2O$. At the lowest concentration employed, elongated particles and some short tetragonal-shaped nanorods of 204 ± 45 nm in diameter and 0.8 ± 0.5 μm long are observed (Fig. 2(a)). When the concentration was raised to 0.113 M, complete development of tetragonal-shaped nanorods was clearly observed (Fig. 2(b)). The product consisted of short nanorods with diameter of 190 ± 8 nm and length of 1.1 ± 0.2 μm aggregating homocentrically to form nanorod cluster of 2.2 ± 0.15 μm in size similar to the structure of an urchin. More well-defined clusters of 2.8 ± 0.15 μm in size made up of longer nanorods (diameter = 190 ± 6 nm, length = 1.4 ± 0.2 μm) was obtained when the concentration was further increased. Detailed analysis of several nanorod clusters by TEM, a typical image shown in Fig. 2(d), clearly revealed that the cluster consists of many nanorods of uniform size and shape having the common point. The selected-area electron diffraction pattern (inset) indicated that the nanorods are single crystalline. This result suggests that the cluster grew via the growth of individual nanorods which grew outwards homocentrically. It is not likely that the cluster is formed by aggregation of the fully grown nanorods. The clusters with longer nanorods obtained at higher concentration of $Na_2SnO_3 \cdot 3H_2O$ can be attributed to the more supersaturated condition attained.

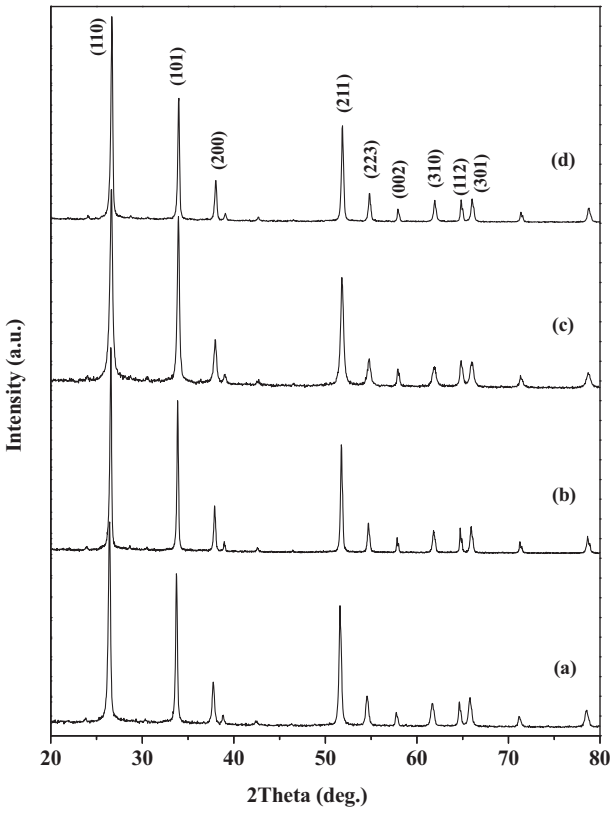

Fig. 1. XRD patterns of SnO_2 nanorod clusters prepared at fixed NaOH concentration of 0.35 M and $Na_2SnO_3 \cdot 3H_2O$ concentration of (a) 0.075 M, (b) 0.113 M, (c) 0.150 M and (d) 0.188 M.

Fig. 3 shows the relationship between the amount of the SnO_2 nanorods and concentration of the $Na_2SnO_3 \cdot 3H_2O$ employed. The amount of SnO_2 increases parabolically with the increase of $Na_2SnO_3 \cdot 3H_2O$ concentration, indicating its significant effect at high concentration. According to the trend in Fig. 3, it is very likely that higher percent yield can be obtained at the concentration higher than 0.188 M. The dramatic increase of hydrothermal product with increasing concentration can be described based on the enhanced solubility of solid precursor. At low $Na_2SnO_3 \cdot 3H_2O$ concentration, the supersaturation regime for crystallization is narrow leading to limited extent of crystal growth. At high $Na_2SnO_3 \cdot 3H_2O$ concentration, this regime can be widen particularly under hydrothermal condition as a result of increased solubility of the solid precursor compared to that

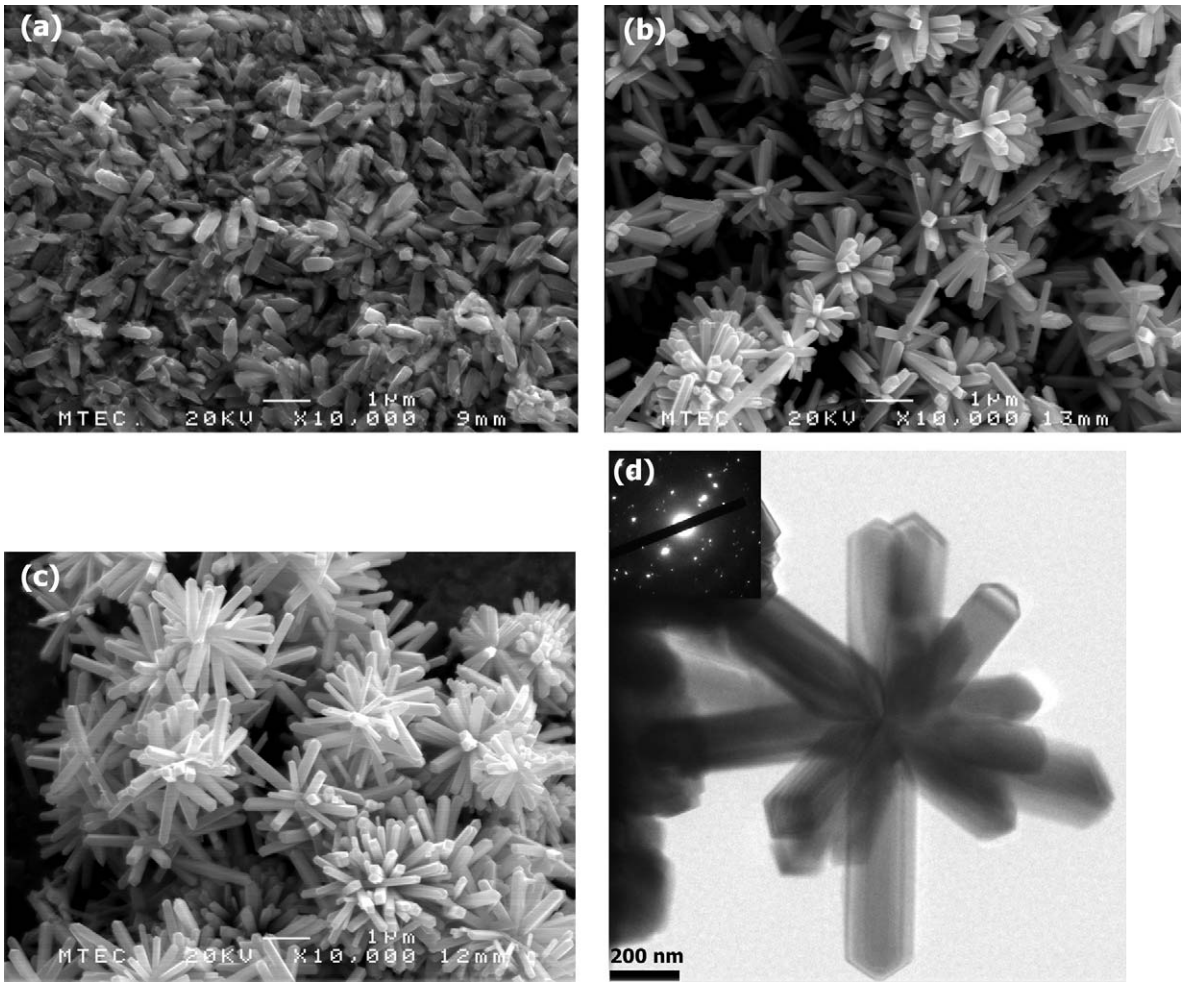

Fig. 2. SEM images of SnO_2 nanorod clusters prepared at fixed NaOH concentration of 0.35 M and $Na_2SnO_3{\cdot}3H_2O$ concentration of (a) 0.075 M, (b) 0.113 M and (c) 0.188 M. TEM image of the cluster obtained from 0.188 M [$Na_2SnO_3{\cdot}3H_2O$]/0.35 M [NaOH] is shown in (d).

at normal condition for a typical chemical synthesis (ambient pressure, temperature < 100 °C).[16] Therefore, numerous nuclei are formed and growth can be at large extent as long as the degree of supersaturation does not fall below the limit for crystal growth.

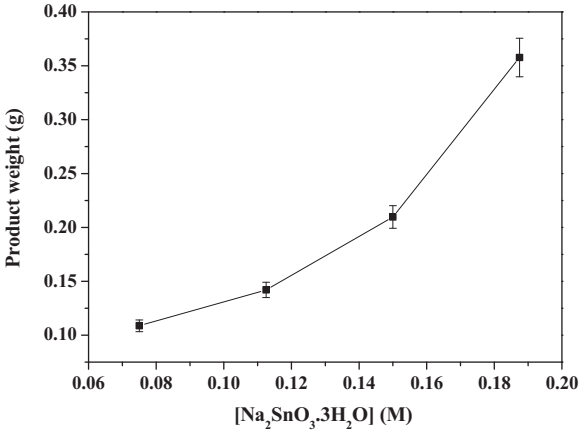

Fig. 3. The amount of SnO_2 product obtained at various concentrations of $Na_2SnO_3{\cdot}3H_2O$ and NaOH concentration of 0.35 M.

It is known that the hydrothermal process takes place through 2 steps: a dissolution and subsequent crystallization. SnO_2 nanorods can be formed through dissolution of the solid precursor followed nucleation when supersaturated concentration at the hydrothermal condition is reached. The increase of percent yield at higher $Na_2SnO_3{\cdot}3H_2O$ concentration can be explained based on the increase of degree of supersaturation (S) which is a ratio of a concentration of the hydrolyzed Sn species and a concentration of the solution in equilibrium with the crystal. In our experiment, higher concentration of $Na_2SnO_3{\cdot}3H_2O$ resulted in more amount of the amorphous precipitate, which consequently resulting in higher concentration of dissolved Sn cation in the hydrothermal solution. The more supersaturated solution leads to more crystallization since it requires lower activation energy for nucleation (ΔG^*) which is defined by[17]:

$$\Delta G^* = \frac{16\pi\sigma^3 M^2}{3(\rho RT \ln S)^2}, \quad (1)$$

where σ is the interfacial tension between the crystal and its surrounding, ρ is the crystal's density and M is the crystal's molecular weight.

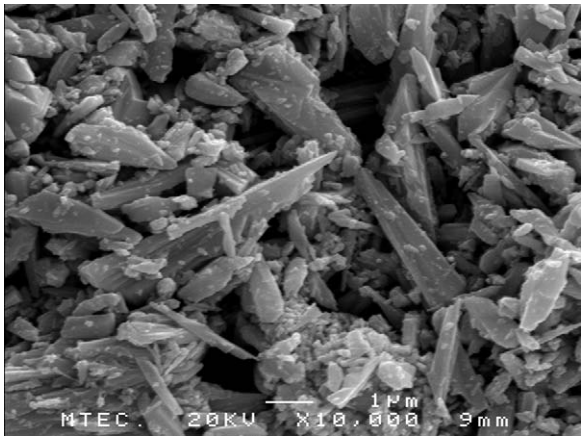

Fig. 4. SEM image of SnO_2 prepared from 0.188 [$Na_2SnO_3{\cdot}3H_2O$]/0.5 M [NaOH].

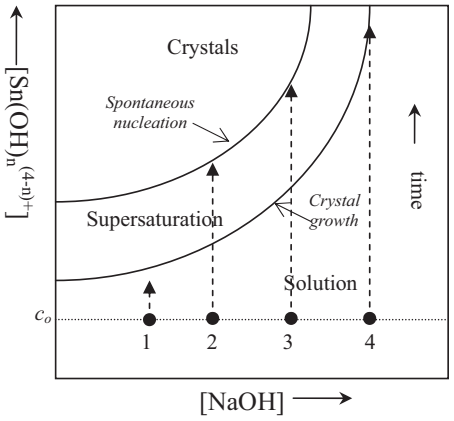

Fig. 5. Schematic illustration of stability diagram of SnO_2 which represents synthesis conditions at various [NaOH] and fixed [$Na_2SnO_3{\cdot}3H_2O$] of 0.188 M.

It should be pointed out that nanorod structure can be developed without the use of shape-forming agents. In our hydrothermal system, at the initial stage, the solid precursor was continuously dissolved in the basic fluid as temperature increased followed by hydrolysis of a dissolved Sn^{4+} resulting in numerous hydrolyzed tin species such as $Sn(OH)^{3+}$, $Sn(OH)_2{}^{2+}$, $Sn(OH)^{3+}$, $Sn(OH)_{4(aq)}$ and $Sn(OH)_6{}^{2-}$.[18] The concentration of these hydrolyzed species increased with time. Once a critical concentration was reached, nuclei were formed and subsequent crystal growth took place.

To investigate the influence of pH of the medium on crystallization of the products, the experiments was carried at fixed $Na_2SnO_3{\cdot}3H_2O$ concentration of 0.188 M and NaOH concentrations of 0.1 M, 0.5 M and 1.0 M instead of 0.35 M as employed in the typical synthesis. The use of 0.1 M and 1.0 M NaOH did not lead to the formation of any type of solid product as no precipitate product was found. The use of 0.5 M NaOH resulted in aggregated SnO_2 nanorods and irregular-shaped SnO_2 as seen in Fig. 4. It is evident from this result that either too low or too high basic concentration was unfavorable for crystallization of

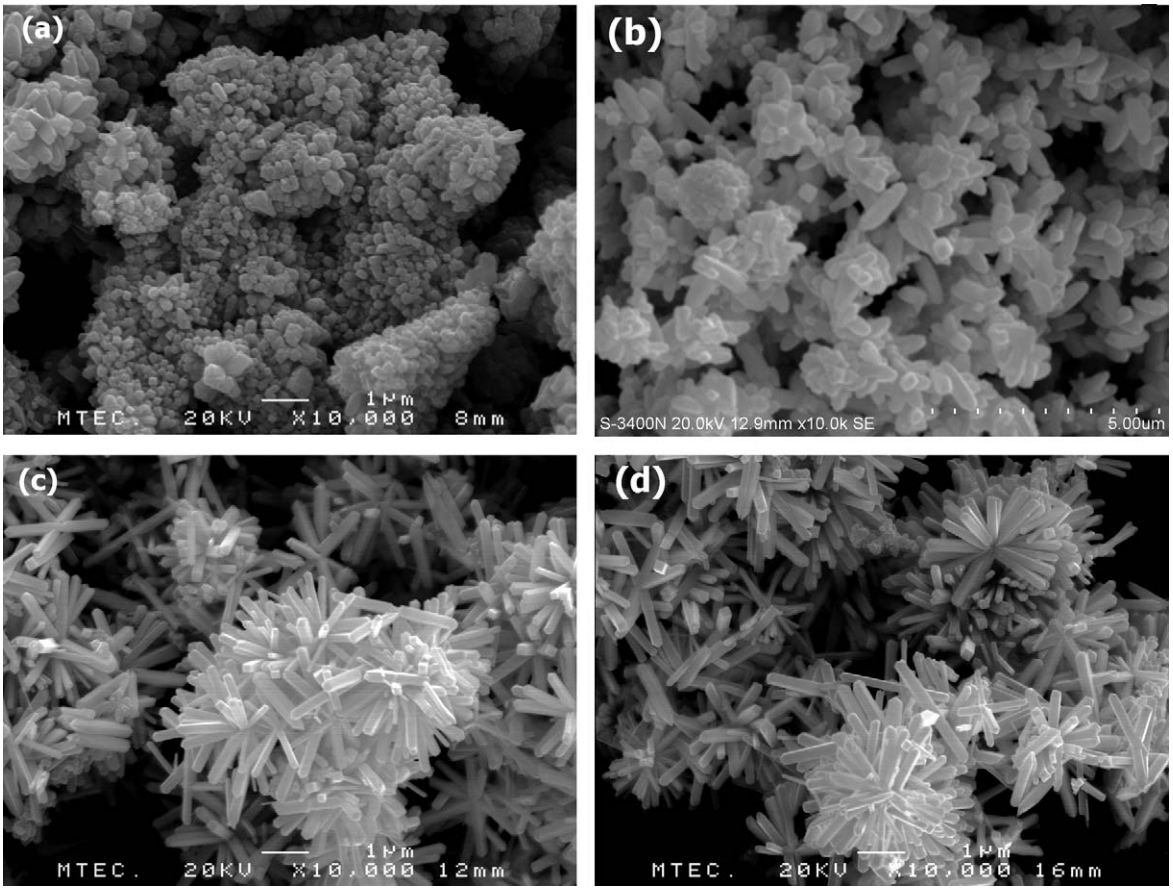

Fig. 6. SEM images of SnO_2 nanorod clusters prepared from 0.188 M [$Na_2SnO_3{\cdot}3H_2O$]/0.35 M [NaOH] at 200 °C for (a) 24 h, (b) 36 h, (c) 48 h and (d) 72 h.

the SnO_2 nanorods. Effect of NaOH concentration on crystallization behavior is schematically shown in Fig. 5 which is a typical stability diagram of metal oxides. Most oxides including SnO_2 are amphoteric as they can be dissolved in both acid and basic media. At high and low pHs, solubility of the oxides is high, and the dissolved hydrolyzed species are their stable phase. As the pH approaching neutral, the stability is decreasing and crystallization can occur provided that the critical concentrations for spontaneous nucleation and growth are satisfied.

At fixed concentration of tin oxide precursor in our hydrothermal fluid, the solid precursor continuously dissolved in the basic medium as the temperature increased resulting in Sn^{4+} solution with concentration of c_o. The Sn^{4+} underwent hydrolysis reaction producing hydrolyzed Sn species (i.e. $Sn(OH)_n^{(4-n)+}$) which resulted in the increase of degree of supersaturation of the solution. It is known that hydroxyl ion (OH^-) plays a significant role in the hydrolysis reaction. At low NaOH concentration (arrow 1, representing 0.188 M [$Na_2SnO_3 \cdot 3H_2O$]/0.10 M [NaOH] solution), total concentration of hydrolyzed Sn species is below the critical concentration for spontaneous nucleation, and therefore nucleation did not occur. At medium NaOH concentration (arrows 2 and 3, representing 0.188 M [$Na_2SnO_3 \cdot 3H_2O$]/0.35 M [NaOH] and 0.188 M [$Na_2SnO_3 \cdot 3H_2O$]/0.5 M [NaOH] solutions, respectively), total concentration of the hydrolyzed Sn species reaches the critical concentration for spontaneous nucleation, and nucleation occurs. A subsequent crystal growth can take place as long as the total concentration is in the supersaturation regime. At high NaOH concentration (arrows 4, representing 0.188 M [$Na_2SnO_3 \cdot 3H_2O$]/1.0 M [NaOH] solution), the hydrolysis occurs at largest extent compared to other conditions resulting in highest total concentration of Sn species. However, the concentration of Sn species is below the critical concentration for spontaneous nucleation, and therefore nucleation did not occur.

In order to reveal formation mechanism of the SnO_2 nanorod clusters, the experiment was carried out at various hydrothermal times and the results are shown in Fig. 6. At the hydrothermal time of 24 h, aggregates of tetragonal-shaped SnO_2 nanocrystals were observed. When the time was prolonged to 36 h, the clusters composing of nanorods with diameters of ~190 nm and lengths of ~1 μm were obtained. The nanorods of the same diameter and length of ~1.4 μm was obtained when the time was 48 h. When the time was prolonged further to 72 h, the nanorod clusters of similar microstructure were obtained indicating that the crystal growth was completed. Based on the above observation, the possible formation mechanism of SnO_2 nanorod clusters can be schematically shown in Fig. 7. Under hydrothermal condition, numerous SnO_2 nuclei were formed rapidly once the critical concentration for spontaneous nucleation was reached. These nuclei grew and aggregated to minimize the total surface area thus minimizing the total interfacial energy. These nanocrystals then grew homocentrically, resulting to the urchin-like clusters. A similar growth mechanism of nanorod clusters via aggregation and Ostwald ripening of nanocrystals followed by their growth is also reported in the synthesis of Zn-doped SnO_2 nanorod clusters.[19]

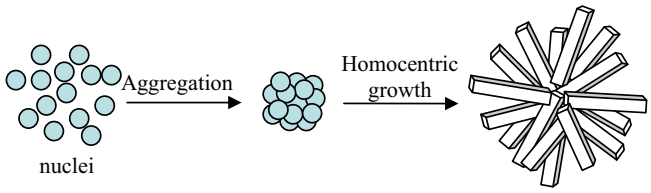

Fig. 7. Schematic illustration describing the growth mechanism of SnO_2 nanorod clusters.

4. Conclusions

SnO_2 nanorod clusters consisting of single crystalline, tetragonal-shaped nanorods have been synthesized by using a simple hydrothermal method without the use of shape-inducing agent. The concentrations of both $Na_2SnO_3 \cdot 3H_2O$ and NaOH strongly affected the formation, morphology and yield of the SnO_2 products. The increase of $Na_2SnO_3 \cdot 3H_2O$ concentration led to more yield and more well-defined, longer nanorods as a result of high degree of supersaturation attained. The effect of NaOH concentration was found to be more complicated. The nanorods were obtained only at moderate concentrations that led to supersaturated solution satisfying nucleation and growth. Too high concentration resulted in stable solution because of amphoteric nature of the SnO_2 while too low concentration resulted in low hydrolysis reaction. Based on the time-dependent study, it is proposed that the nanorod clusters were formed via the aggregation of SnO_2 nanocrystals followed by their homocentric growth.

Acknowledgements

The authors would like to acknowledge the financial support from the National Metal and Materials Technology Center, Thailand (Grant# MT-B-52-CER-07-230-I).

References

1. Seiyama T, Kato A, Fujushi K, Nagatani M. A new detector for gaseous components using semiconductive thin films. *Analytical Chemistry* 1962;**34**, 1502f.
2. Tamaki J, Nakataya Y, Konishi S. Micro gap effect on dilute H_2S sensing properties of SnO_2 thin film microsensors. *Sensors and Actuators* 2008;**B130**:400–4.
3. Supothina S. Gas sensing properties of nanocrystalline SnO_2 thin films prepared by liquid flow deposition. *Sensors and Actuators* 2003;**B93**: 526–30.
4. Kim HR, Choi KI, Lee JH, Akbar SA. Highly sensitive and ultra-fast responding gas sensors using self-assembled hierarchical SnO_2 spheres. *Sensors and Actuators* 2009;**B136**:138–43.
5. Jiaqiang X, Ding W, Lipeng Q, Weijun Y, Qingyi P. SnO_2 nanorods and hollow spheres: controlled synthesis and gas sensing properties. *Sensors and Actuators* 2009;**B137**:490–5.
6. Kolmakov A, Zhang Y, Cheng G, Moskovits M. Detection of CO and O_2 using tin oxide nanowire sensors. *Advanced Materials* 2003;**15**: 997–1000.
7. Wang Y, Lee JY, Zeng HC. Polycrystalline SnO_2 nanotubes prepared via infiltration casting of crystallites and their electrochemical application. *Chemistry of Materials* 2005;**17**:3899–903.
8. Firooz AA, Mahjoub AR, Khodadadi AA. Highly sensitive CO and ethanol nanoflower-like SnO_2 sensor among various morphologies obtained by

using single and mixed ionic surfactant templates. *Sensors and Actuators* 2009;**B141**:89–96.
9. Ho SY, Wong ASW, Ho GW. Controllable porosity of monodispersed tin oxide nanosphere via an additive-free chemical route. *Crystal Growth & Design* 2009;**9**:732–6.
10. Ba JH, Polleux J, Antonietti M, Niederberger M. Non-aqueous synthesis of tin oxide nanocrystals and their assembly into ordered porous mesostructures. *Advanced Materials* 2005;**17**:2509–12.
11. Kim HW, Shim SH. Synthesis and characteristics of SnO_2 needle-shaped nanostructures. *Journal of Alloys and Compounds* 2006;**426**:286–9.
12. Xu C, Xu G, Liu Y, Zhao X, Wang G. Preparation and characterization of SnO_2 nanorods by thermal decomposition of SnC_2O_4 precursor. *Scripta Materialia* 2002;**46**:789–94.
13. Wang DW, Chu X, Gong M. Gas-sensing properties of sensors based on single-crystalline SnO_2 nanorods prepared by a simple molten-salt method. *Sensors and Actuators* 2006;**B117**:183–7.
14. Gao T, Wang T. Sonochemical synthesis of SnO_2 nanobelt/CdD nanoparticle core/shell heterostructures. *Chemical Communications* 2004;**22**:2558–9.
15. Lupan O, Chow L, Chai G, Heinrich H, Park S, Schulte. A. Synthesis of one-dimensional SnO_2 nanorods via a hydrothermal technique. *Physica* 2009;**E41**:533–6.
16. Schäf O, Ghobarkar H, Knauth P. Hydrothermal synthesis of nanomaterials. In: Knauth P, Schoonman J, editors. *Nanostructured materials: selected synthesis methods, properties and applications*. London: Kluwer Academic Publishers; 2002. pp. 23–41.
17. Mullin JW. *Crystallization*. Oxford: Butterworth-Heinemann; 2001.
18. Baes CF, Mesmer RE. *The hydrolysis of cations*. New York: John Wiley & Sons; 1986.
19. Ding X, Zeng D, Xie C. Controlled growth of SnO_2 nanorods clusters via Zn doping and its influence on gas-sensing properties. *Sensors and Actuators* 2010;**B149**:336–44.